



 Cite this: *RSC Adv.*, 2019, 9, 10320

 Received 25th February 2019  
Accepted 26th March 2019

DOI: 10.1039/c9ra01427f

[rsc.li/rsc-advances](http://rsc.li/rsc-advances)

# Facile preparation of low-cost HKUST-1 with lattice vacancies and high-efficiency adsorption for uranium

 Aili Yang, \* Ping Li and Jingrong Zhong

In this work, we prepared HKUST-1 and HKUST-1 with lattice vacancies (HLV) using benzoic acid (BA) as a low-cost modulator to replace part of the traditional trimesic acid ligand ( $H_3BTC$ ). The structure and morphology of the products were characterized by FTIR, XRD, SEM and XPS. The adsorption performance of the products for uranium from aqueous solutions was investigated. The results showed that the sorption of  $U(VI)$  on HKUST-1 and HLV agreed with the Langmuir isotherm model ( $R_{HKUST-1}^2 = 0.9867$  and  $R_{HLV}^2 = 0.9828$ ) and the maximum adsorption capacity was  $430.98 \text{ mg g}^{-1}$  and  $424.88 \text{ mg g}^{-1}$ , respectively. According to kinetics studies, the adsorption fitted better with a pseudo-second-order model ( $R_{HKUST-1}^2 = 1.0000$  and  $R_{HLV}^2 = 0.9978$ ). The as-prepared adsorbents were used for the removal of uranium from real water samples as well. The results showed that HLV with lower cost is a promising adsorbent for uranium from aqueous solutions.

## 1. Introduction

Nowadays, there is a growing interest in the development and applications of various nanostructured materials in many fields.<sup>1</sup> Various materials including organic complexes,<sup>2</sup> inorganic nanocomposites,<sup>3,4</sup> and polyelectrolytes/anions<sup>5</sup> have been applied for contamination removal. Recently, metal-organic frameworks (MOFs) have become a new promising nanostructured material. MOFs are crystalline porous materials comprised of metal ions linked by various organic bridges. MOFs with large specific surface areas, high porosity, tuneable pore sizes and adjustable internal surfaces have been widely applied in various fields, such as gas storage and separation,<sup>6,7</sup> catalysis,<sup>8,9</sup> supercapacitor fabrication<sup>10</sup> and adsorption of undesirable materials.<sup>11–13</sup> Among various wastewater treatment technologies adsorption is considered the best and most universal technique for the removal of a wide variety of organic and inorganic pollutants.<sup>14</sup> Because of its excellent chemical and thermal stability,<sup>15,16</sup> HKUST-1 is a typical material among MOFs and has been intensively investigated for the removal of various pollutants, such as  $H_2S$ ,<sup>17</sup>  $Pb(II)$ ,<sup>18</sup> dyes,<sup>19,20</sup>  $Cr^{2+}$ ,<sup>21</sup>  $Ni(II)$ ,<sup>22</sup>  $As(V)$ ,<sup>23</sup>  $Cr(VI)$ ,<sup>24</sup> hydroquinone,<sup>25</sup> fluoroquinolone,<sup>26</sup> pesticides<sup>27,28</sup> and uranium.<sup>29,30</sup>

In general, trimesic acid ( $H_3BTC$ ) has been used as the traditional ligand to prepare HKUST-1 in the previous reports. However, the cost of  $H_3BTC$  (the cost of analytical grade product is currently 566 ¥/500 g) is much higher than that of benzoic acid (BA) with less  $-COOH$  groups (the cost of analytical grade product is currently 16.4 ¥/250 g). The preparation cost of

HKUST-1 will greatly reduce by using BA as the ligand to replace part of  $H_3BTC$ . To the best of our knowledge, no reports have been published about the preparation and adsorption capacity of HKUST-1 using low-cost BA as the modulator for uranium from aqueous solutions. Therefore, to reduce significantly the preparation cost of HKUST-1, we used BA to replace part of the traditional  $H_3BTC$  ligand to obtain HKUST-1 with lattice vacancies (HLV). Moreover, the as-synthesized HKUST-1 and HLV in the present work have another two advantages: (1) the removal rate of uranium using HKUST-1 and HLV reached 99% even for the solutions bearing a high concentration of uranium ( $100 \text{ mg L}^{-1}$ ), and (2) the maximum adsorption capacity of HKUST-1 and HLV were up to about 431 and  $425 \text{ mg g}^{-1}$ , respectively, which was higher than most of the reported references (see Table 3). Herein, we prepared HKUST-1 and HLV by a simple hydrothermal synthesis method for the adsorption of uranium from aqueous solutions. The influence of solution pH, co-existing ions, contact time, and initial  $U(VI)$  concentration on the adsorption capacity was studied. The adsorption isotherms and kinetics models were also investigated.

## 2. Materials and methods

### 2.1. Materials

Stock solutions of uranium ( $5\text{--}100 \text{ mg L}^{-1}$ ) were prepared by dissolving  $UO_2(NO_3)_2 \cdot 6H_2O$  (Xi'an Dingtian Chemical Reagent Co.) in deionized water (DW) and acidified with a small amount of concentrated  $HNO_3$ . All the chemicals, *i.e.*,  $Cu(NO_3)_2 \cdot 3H_2O$ ,  $H_3BTC$ , BA and absolute ethanol, were of analytical grade and used without further purification. DW was used throughout the experiments.

Institute of Materials, China Academy of Engineering Physics, Huafeng Xincun No. 9  
Mail-box 9071-7, Jiangyou, 621900, China. E-mail: yang770117@sina.com



## 2.2. Preparation of HKUST-1 and HLV

The preparation method of HKUST-1 and HLV was modified according to the ref. 31. In a typical synthesis of HKUST-1, 1.0870 g of  $\text{Cu}(\text{NO}_3)_2 \cdot 3\text{H}_2\text{O}$  was dissolved in 15 ml DW, while 0.5250 g of  $\text{H}_3\text{BTC}$  was dissolved in 15 ml absolute ethanol. Both solutions were mixed and stirred for 30 min. The resulting mixture was transferred into a Teflon autoclave and heated in an oven at 110 °C for 24 h. The resultant blue crystals were filtered under vacuum and washed with ethanol and DW ( $v : v = 1 : 1$ ) and ethanol. Then, the products were immersed in ethanol for 36 h and ethanol was replaced every 12 h. Finally, the products were filtered under vacuum and dried at 100 °C under vacuum.

In a typical synthesis of HLV, 1.0870 g of  $\text{Cu}(\text{NO}_3)_2 \cdot 3\text{H}_2\text{O}$  was dissolved in 15 ml DW. The mixture of  $\text{H}_3\text{BTC}$  and BA with molar ratio 3 : 1 was dissolved in 15 ml absolute ethanol. Then, both solutions were transferred into a Teflon autoclave and heated in an oven at 110 °C for 24 h. The resultant blue crystals were filtered under vacuum and washed with a solution of ethanol and DW ( $v : v = 1 : 1$ ) and ethanol. Then, the products were immersed in ethanol for 36 h and ethanol was replaced every 12 h. Finally, the products were filtered under vacuum and dried at 100 °C under vacuum.

## 2.3. Characterization of the products

The Fourier transform infrared (FTIR) spectra of the as-prepared adsorbents were obtained using an FTIR spectrometer (Bruker VERTEX 70, Germany). The crystal phases of the samples were characterized by X-ray diffraction (XRD) pattern (Dandong Fangyuan DX-2700 model, China). The surface morphology of the products was determined using scanning electron microscopy (SEM) (FEI Helios 600i, USA). X-ray photoelectron spectroscopy (XPS) was used to analysis the elemental content of HKUST-1 and HLV using an ESCALAB 250 X-ray photoelectron spectrometer (Thermo Fisher, USA).

## 2.4. Adsorption tests

The influences of pH, contact time and initial uranium concentration on the removal efficiency of uranium were investigated by batch adsorption experiments. The solution pH was adjusted by NaOH and HCl. The as-prepared adsorbent was added to a 20 ml  $\text{U}(\text{vi})$  solution and shaken in a shaker (Kangshi, China). After filtration, residual uranium concentrations were measured by a micro-quantity uranium analyser (MUA model, China). The removal rate  $R$  (%) and the adsorption capacity of  $\text{U}(\text{vi})$   $Q$  ( $\text{mg g}^{-1}$ ) were calculated according to eqn (1) and (2), respectively.

$$R(\%) = \frac{c_0 - c_t}{c_0} \times 100 \quad (1)$$

$$Q(\text{mg g}^{-1}) = \frac{(c_0 - c_t)}{W} \times V \quad (2)$$

where  $c_0$  ( $\text{mg L}^{-1}$ ) is the initial  $\text{U}(\text{vi})$  concentration,  $c_t$  ( $\text{mg L}^{-1}$ ) is  $\text{U}(\text{vi})$  concentration at time  $t$ ,  $V$  (L) is the solution volume and  $W$  (g) is the weight of adsorbent.

## 3. Results and discussion

### 3.1. Characterization of the products

The functional group structures of HKUST-1 and HLV were determined by FTIR and are shown in Fig. 1. The characteristic peak at  $1370 \text{ cm}^{-1}$  was assigned to the C–O of  $\text{H}_3\text{BTC}$ , and the bands at  $1448 \text{ cm}^{-1}$  and  $1549 \text{ cm}^{-1}$  were attributed to the C=O of  $\text{H}_3\text{BTC}$ . The characteristic peak at  $1647 \text{ cm}^{-1}$  resulted from aromatic C=C of  $\text{H}_3\text{BTC}$ . This result is in accordance with a previous study.<sup>31,32</sup> However, in the HLV FTIR spectrum, the intensity of the  $\text{H}_3\text{BTC}$  characteristic peaks at  $1448 \text{ cm}^{-1}$  and  $1549 \text{ cm}^{-1}$  attributed to C=O and the –OH group at  $>3000 \text{ cm}^{-1}$  decreased significantly because part of the  $\text{H}_3\text{BTC}$  was replaced by BA in the HLV, which has fewer –COOH groups than  $\text{H}_3\text{BTC}$ . Moreover, by XPS elemental analysis the calculated atomic ratio of C : Cu : O in HKUST-1 and HLV is 8.37 : 1 : 4.73 and 7.22 : 1 : 4.25, respectively, which indicated that the part of  $\text{H}_3\text{BTC}$  was replaced by BA with less –COOH groups in HLV.

The XRD patterns of the resulting HKUST-1 and HLV are shown in Fig. 2. All of the diffraction peaks of HKUST-1 were in accordance with those reported in the ref. 29, and the indexed values of all of the diffraction peaks were accordance with the reference.<sup>33–35</sup> Fig. 2 shows that the crystalline structure of HKUST-1 was similar to that of HLV. No obvious impurity peaks can be detected in the XRD patterns of HKUST-1 and HLV. The results showed that HKUST-1 and HLV had good chemical

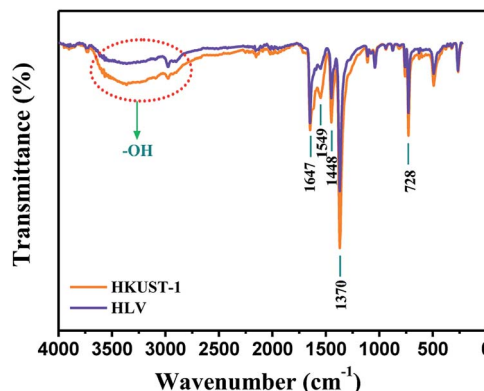


Fig. 1 FTIR spectra of HKUST-1 and HLV.

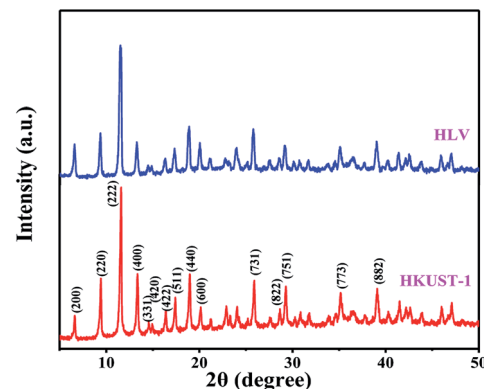


Fig. 2 XRD patterns of HKUST-1 and HLV.



stability and high crystallinity even if the part of H<sub>3</sub>BTC was replaced by BA.<sup>36</sup>

The morphology of HKUST-1 and HLV are shown in Fig. 3. In the SEM of HKUST-1, the crystal sizes of tens of microns (Fig. 3a) were observed. Some of the particles were octahedra with clear edges, and the other particles were flower-like (Fig. 3b). Due to the replacement by BA, the pores in HLV were deeper than those in HKUST-1.

### 3.2. Effect of pH and co-existing ions on adsorption

The adsorption of U(vi) by HKUST-1 and HLV as a function of pH was carried out over the pH range of 3.0–8.0 for 30 min, as shown in Fig. 4, and the effect of co-existing ions on U(vi) adsorption was shown in Fig. 4 (inset). The results showed a significant impact of pH on uranium adsorption. The highest removal rate of U(vi) was observed at pH 4.0 and was found to be nearly 100%. The observed lower removal efficiency of U(vi) at pH < 3 may be attributed to formation of repulsive force between the protonated adsorbent and the positively charged uranyl ions which hindered the mass transfer and their adsorption onto the adsorbent. With the increase of pH

deprotonation of HKUST-1 and HLV cause enhance in the complex formation and improvement in mass transfer to the adsorbent surface.<sup>37,38</sup> However, at pH > 5 the interaction of U(vi) with HKUST-1 and HLV decreased due to the formation of uranyl species with low adsorption affinities, such as  $[\text{UO}_2\text{OH}]^+$ ,  $[(\text{UO}_2)_3(\text{OH})_4]^{2+}$ ,  $[(\text{UO}_2)_3(\text{OH})_5]^{2+}$ ,  $[(\text{UO}_2)_2(\text{OH})_2]^{2+}$ ,  $[(\text{UO}_2)_2\text{OH}]^{3+}$ ,  $[(\text{UO}_2)_3(\text{OH})]^{5+}$ , and  $[(\text{UO}_2)_4(\text{OH})]^{7+}$ .<sup>39</sup> Therefore, the optimum pH of HKUST-1 and HLV for U(vi) adsorption was 4.0. Moreover, the effect of co-existing ions ( $\text{K}^+$ ,  $\text{Mg}^{2+}$ ,  $\text{Ca}^{2+}$ ,  $\text{Al}^{3+}$  and  $\text{Sr}^{2+}$ ) on U(vi) sorption is examined. As shown in Fig. 4 (inset), some co-existing ions (such as  $\text{Mg}^{2+}$  and  $\text{Ca}^{2+}$ ) had significantly effect on the adsorption efficiency for U(vi) by HLV at pH 4 while some ions (such as  $\text{Al}^{3+}$  and  $\text{Sr}^{2+}$ ) had no effect on the adsorption efficiency for U(vi).

### 3.3. Influence of contact time and adsorption kinetics study

Fig. 5a shows the effect of contact time on uranium adsorption by HKUST-1 and HLV. The adsorption efficiency of HKUST-1

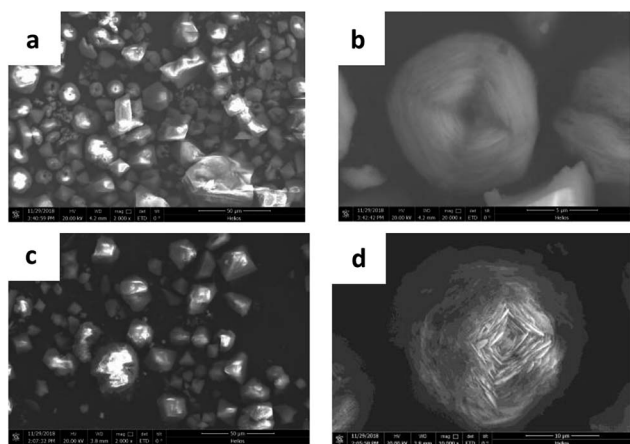


Fig. 3 SEM of HKUST-1 ((a) 2000 $\times$  and (b) 20 000 $\times$ ) and HLV ((c) 2000 $\times$  and (d) 10 000 $\times$ ).

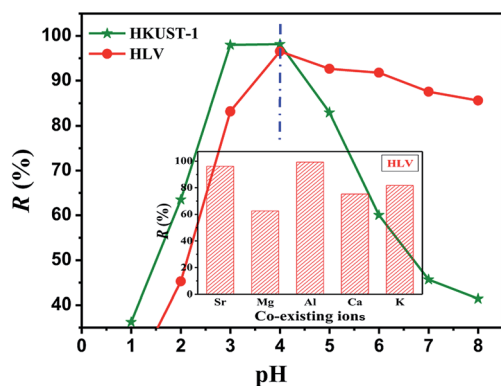


Fig. 4 Effect of pH on U(vi) adsorption by HKUST-1 and HLV; the inset is the effect of co-existing ions on the removal of U(vi) by HLV.  $C_{(\text{U})\text{initial}} = 10 \text{ mg L}^{-1}$ ,  $m/V = 0.25 \text{ g L}^{-1}$ , and contact time = 30 min.

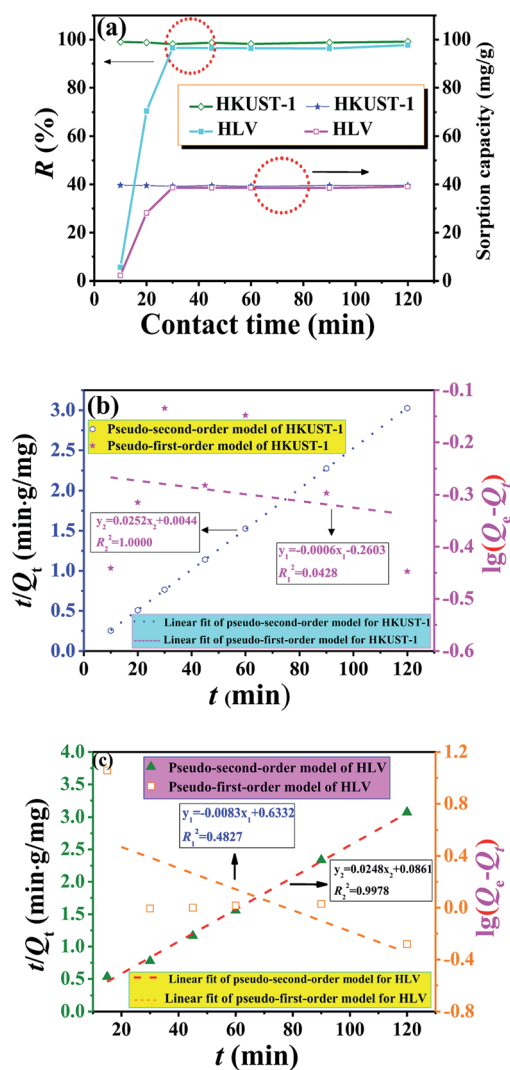


Fig. 5 (a) Influence of contact time on U(vi) adsorption, (b) kinetics model fits of HKUST-1 and (c) kinetics model fits of HLV. pH = 4.0,  $C_{(\text{U})\text{initial}} = 10 \text{ mg L}^{-1}$ , and  $m/V = 0.25 \text{ g L}^{-1}$ .



**Table 1** Parameters of pseudo-first-order and pseudo-second-order kinetic models for U(vi) adsorption by HKUST-1 and HLV. pH = 4.0,  $C_{(U)initial} = 10 \text{ mg L}^{-1}$ ,  $m/V = 0.25 \text{ g L}^{-1}$

Sorbents	Pseudo-first-order model			Pseudo-second-order model		
	$Q_e \text{ (mg g}^{-1}\text{)}$	$k_1 \text{ (min}^{-1}\text{)}$	$R^2$	$Q_e \text{ (mg g}^{-1}\text{)}$	$k_2 \text{ (g (mg}^{-1} \text{ min}^{-1}\text{))}$	$R^2$
HKUST-1	0.5492	0.0014	0.0428	39.6825	0.1443	1.0000
HLV	4.2973	0.0191	0.4827	40.3226	0.0071	0.9978

and HLV improved significantly with time and reached adsorption equilibrium within 30 min. The removal rates of uranium of HKUST-1 and HLV were up to ~99%. The linear fit of pseudo-first-order and pseudo-second-order kinetic models for U(vi) adsorption by HKUST-1 and HLV is shown in Fig. 5b and c, and the calculated fit parameters according to eqn (3) and (4)<sup>40</sup> are given in Table 1. The correlation coefficient of the pseudo-second-order model ( $R^2 = 1.0000$  for HKUST-1 and  $R^2 = 0.9978$  for HLV) was superior to that of the pseudo-first-order model, which indicated that the adsorption of U(vi) onto HKUST-1 and HLV fit the pseudo-second-order model well. The fit results demonstrated that the chemical interactions played a significant role in the rate-controlling steps. The equations are as follows:

$$\lg(Q_e - Q_t) = \lg Q_e - \frac{k_1}{2.303} t \quad (3)$$

$$\frac{t}{Q} = \frac{1}{k_2 Q_e^2} + \frac{t}{Q_e} \quad (4)$$

where  $k_1 \text{ (min}^{-1}\text{)}$  is the Lagergren rate constant of adsorption and  $k_2 \text{ (g (mg}^{-1} \text{ min}^{-1}\text{))}$  is the rate constant of pseudo-second-order adsorption.

### 3.4. Adsorption isotherm

The Langmuir and Freundlich isotherm models are expressed in eqn (5) and (6),<sup>40</sup> respectively, and the calculated Langmuir and Freundlich isotherm fit data of HKUST-1 and HLV are shown in Table 2. It is clear from Fig. 6 that the equilibrium adsorption for HKUST-1 and HLV fit well to the Langmuir model, and the correlation coefficients of HKUST-1 and HLV were 0.9867 and 0.9828, respectively. The maximum adsorption capacity ( $Q_m$ ) of HKUST-1 and HLV for U(vi) reached  $430.98 \text{ mg g}^{-1}$  and  $424.88 \text{ mg g}^{-1}$ , respectively. Though HLV has more lattice vacancies than that of HKUST-1 because of the replacement by BA, the  $Q_m$  of HKUST-1 was higher than that of HLV, which showed that the adsorption mechanism was mainly the surface complexation and not the increase of active sites.

$$Q_e = \frac{Q_m K_L C_e}{1 + K_L C_e} \quad (5)$$

$$Q_e = K_F C_e^{1/n} \quad (6)$$

where  $Q_e \text{ (mg g}^{-1}\text{)}$  is the equilibrium adsorption capacity,  $C_e \text{ (mg L}^{-1}\text{)}$  is the uranium concentration at equilibrium,  $Q_m \text{ (mg g}^{-1}\text{)}$  is the maximum adsorption capacity,  $K_L \text{ (L mg}^{-1}\text{)}$  and  $K_F \text{ (mg}^{1-n} \text{ L}^n \text{ g}^{-1}\text{)}$  are the Langmuir constant and Freundlich constant, respectively, and  $n$  is the Freundlich adsorption exponent.

A comparison of  $Q_m$  of HKUST-1 and HLV in this work and the reported other adsorbents is presented in Table 3. Table 3 shows that as-prepared low-cost HLV had higher  $Q_m$  than most of the reported adsorbents and proved to be a promising adsorbent for the treatment of uranium-bearing wastewater.

### 3.5. Adsorption efficiency for real wastewater samples

Under the optimum adsorption conditions, the removal efficiency of U(vi) by HKUST-1 and HLV for low-level uranium-

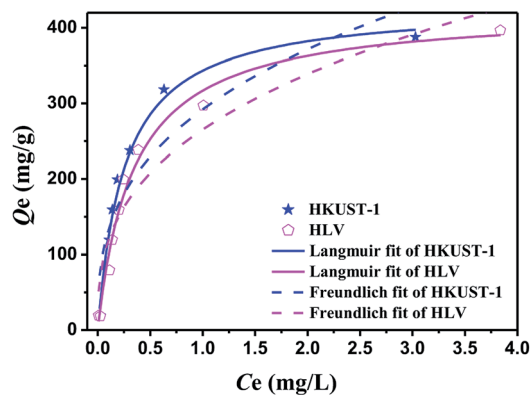


**Fig. 6** Linear fit of Langmuir and Freundlich isotherm models of HKUST-1 and HLV. pH = 4.0,  $C_{(U)initial} = 5\text{--}100 \text{ mg L}^{-1}$ ,  $m/V = 0.25 \text{ g L}^{-1}$ , and contact time = 24 h.

**Table 2** Langmuir and Freundlich model parameters for uranium adsorption on HKUST-1 and HLV. pH = 4.0,  $C_{(U)initial} = 10 \text{ mg L}^{-1}$ ,  $m/V = 0.25 \text{ g L}^{-1}$  and contact time = 24 h

Sorbents	Langmuir model			Freundlich model		
	$Q_m \text{ (mg g}^{-1}\text{)}$	$k_L \text{ (L mg}^{-1}\text{)}$	$R^2$	$n$	$k_F \text{ (mg}^{1-n} \text{ L}^n \text{ g}^{-1}\text{)}$	$R^2$
HKUST-1	430.98	3.9203	0.9867	2.88	292.13	0.8408
HLV	424.88	2.9348	0.9828	2.84	265.30	0.8972



Table 3 Maximum adsorption capacity of various adsorbents for U(VI) ions

Sorbents	pH	$m/V$ (g L <sup>-1</sup> )	$Q_m$ (mg g <sup>-1</sup> )	References
Modified aluminosilica	3.5	1.0	83.30	39
Modified red muds	3.0	3.5	124.56	41
Br-PADAP-impregnated MWCNTs	6.3	0.1	83.40	42
MNPs@PAO	6.0	0.5	216.45	43
Polypyrrole	5.0	1.0	87.72	44
<i>Pseudomonas monteilii</i>	6.0	0.3	267.30	45
AO-MWCNTs	5.0	1.0	67.90	46
Tetraphenylimidodiphosphate	4.5	0.5	99.86	47
HKUST-1	6.0	0.4	787.40	29
HKUST-1@H <sub>3</sub> PW <sub>12</sub> O <sub>40</sub>	6.0	0.2	14.58	30
HKUST-1	4.0	0.25	430.98	This work
HLV	4.0	0.25	424.88	This work

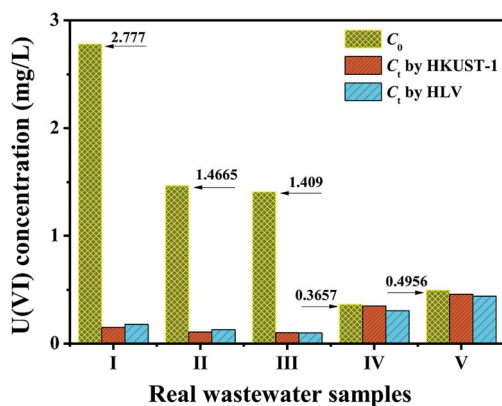


Fig. 7 Column chart of the adsorption efficiency of HKUST-1 and HLW for real uranium-bearing nuclear waste effluents. pH = 4.0,  $C_{(U)}^{\text{initial}} = 0.3\text{--}3.0$  mg L<sup>-1</sup>,  $m/V = 0.25$  g L<sup>-1</sup>, and contact time = 30 min.

bearing real wastewater from five different batches was evaluated. Some micro-quantity metal ions (*e.g.*, Al, B, Ca, Be, Fe, Cu, Mn, Mg, Si, Ni and Mo) were found to exist in the real wastewater samples. All elements in real samples were analyzed by inductively coupled plasma-atomic emission spectrometry (ICP-AES) (Thermo Fisher iCAP 6300, USA). The adsorption experiments results are presented in Fig. 7. As shown in Fig. 7, HKUST-1 and HLW had favourable adsorption capacity for high-level uranium-bearing wastewater ( $>1.0$  mg L<sup>-1</sup>), and the co-existing ions had no effect on the removal efficiency for uranium. However, the uranium concentration after treatment with HKUST-1 and HLW was not significantly reduced when the uranium concentration was very low.

## 4. Conclusions

In this work, HKUST-1 and HLW were synthesized in a facile manner by hydrothermal methods and exhibited high-efficiency adsorption capacity for uranium from aqueous solutions, especially high-level uranium-containing wastewater. The optimal adsorption conditions included a pH of 4.0,  $0.25$  g L<sup>-1</sup> of adsorbent dose and 30 min of contact time when the initial

uranium concentration was  $10$  mg L<sup>-1</sup>. The effect of co-existing ions ( $K^+$ ,  $Mg^{2+}$ ,  $Ca^{2+}$ ,  $Al^{3+}$  and  $Sr^{2+}$ ) on the uranium removal by HLW was studied. Results showed that some co-existing ions (such as  $Mg^{2+}$  and  $Ca^{2+}$ ) had significantly effect on the adsorption efficiency for U(VI) by HLW at pH 4 while some ions (such as  $Al^{3+}$  and  $Sr^{2+}$ ) had no effect on the adsorption efficiency for U(VI). The adsorption processes of HKUST-1 and HLW were well described by the Langmuir isotherm model and pseudo-second-order kinetic model. The maximum adsorption capacities of HKUST-1 and HLW were  $430.98$  and  $424.88$  mg g<sup>-1</sup>, respectively, which is much higher than that of other reported adsorbents. Moreover, HKUST-1 and HLW exhibited favorable adsorption performance for real U(VI)-bearing wastewater samples in practical application. Compared with HKUST-1, low-cost HLW is a very promising potential adsorbent for the removal of uranium from aqueous solutions.

## Conflicts of interest

There are no conflicts to declare.

## Acknowledgements

This work is financially supported by National Natural Science Foundation of China (21407132) and Environmental Protection Foundation of China Academy of Engineering Physics (YAHZY-2018-008).

## References

- 1 A. M. Alansi, W. Z. Alkayali, M. H. Al-qunaibit, T. F. Qahtan and T. A. Saleh, *RSC Adv.*, 2015, 5(87), 71441–71448.
- 2 R. Soury, M. Jabli, T. A. Saleh, W. S. Abdul-Hassan, E. Saint-Aman, F. Loiseau, C. Philouze and H. Nasri, *RSC Adv.*, 2018, 8(36), 20143–20156.
- 3 M. M. Al-Shalalfah, T. A. Saleh and A. A. Al-Saadi, *RSC Adv.*, 2016, 6(79), 75282–75292.
- 4 H. A. Sani, M. B. Ahmad and T. A. Saleh, *RSC Adv.*, 2016, 6(110), 108819–108827.
- 5 Z. A. Jamiu, T. A. Saleh and S. A. Ali, *RSC Adv.*, 2015, 5(53), 42222–42232.



- 6 J. M. Yu, L. H. Xie, J. R. Li, Y. G. Ma, J. M. Seminario and P. B. Balbuena, *Chem. Rev.*, 2017, **117**, 9674–9754.
- 7 K. Xie, Q. Fu, C. L. Xu, H. Lu, Q. H. Zhao, R. Curtain, D. Y. Gu, P. A. Webley and G. G. Qiao, *Energy Environ. Sci.*, 2018, **11**, 544–550.
- 8 R. V. Jagadeesh, K. Murugesan, A. S. Alshammari, H. Neumann, M. M. Pohl, J. Radnik and M. Beller, *Science*, 2017, **358**, 326–332.
- 9 M. M. Wan, X. L. Zhang, M. Y. Li, B. Chen, J. Yin, H. C. Jin, L. Lin, C. Chen and N. Zhang, *Small*, 2017, **13**, 1701395.
- 10 D. Sheberla, J. C. Bachman, J. S. Elias, C. J. Sun, Y. Shao-Horn and M. Dincă, *Nat. Mater.*, 2017, **16**, 220–225.
- 11 Y. H. Pi, X. Y. Li, Q. B. Xia, J. L. Wu, Y. W. Li, J. Xiao and Z. Li, *Chem. Eng. J.*, 2018, **337**, 351–371.
- 12 N. A. A. Qasem, R. Ben-Mansour and M. A. Habib, *Appl. Energy*, 2018, **210**, 317–326.
- 13 D. Bahamon, A. Díaz-Márquez, P. Gamallo and L. F. Vega, *Chem. Eng. J.*, 2018, **342**, 458–473.
- 14 V. K. Gupta, I. Ali, T. A. Saleh, A. Nayak and S. Agarwal, *RSC Adv.*, 2012, **2**(16), 6380–6388.
- 15 L. H. Wee, M. R. Lohe, N. Janssens, S. Kaskel and J. A. Martens, *J. Mater. Chem.*, 2012, **22**, 13742–13746.
- 16 C. Volkringer, C. Falaise, P. Devaux, R. Giovine, V. Stevenson, F. Pourpoint, O. Lafon, M. Osmond, C. Jeanjacques, B. Marcillaud, J. C. Sabroux and T. Loiseau, *Chem. Commun.*, 2016, **52**, 12502–12505.
- 17 H. Y. Zhang, Z. R. Zhang, C. Yang, L. X. Ling, B. J. Wang and H. L. Fan, *J. Inorg. Organomet. Polym. Mater.*, 2018, **28**, 694–701.
- 18 W. X. Yang, J. Wang, Q. F. Yang, H. N. Pei, N. Hu, Y. R. Suo, Z. H. Li, D. H. Zhang and J. L. Wang, *Chem. Eng. J.*, 2018, **339**, 230–239.
- 19 H. M. Abd El Salam and T. Zaki, *Inorg. Chim. Acta*, 2018, **471**, 203–210.
- 20 N. Chen, N. D. Chen, F. H. Wei, S. Q. Zhao and Y. Luo, *Chem. Phys. Lett.*, 2018, **705**, 23–30.
- 21 S. Yekta and M. J. Sadeghi, *J. Inorg. Organomet. Polym. Mater.*, 2018, **28**, 1049–1064.
- 22 M. R. Faradonbeh, A. A. Dadkhah, A. Rashidi, S. Tasharofi and F. Mansourkhani, *J. Inorg. Organomet. Polym. Mater.*, 2018, **28**, 829–836.
- 23 C. Zhang, Y. Xiao, Y. Qin, Q. C. Sun and S. H. Zhang, *J. Solid State Chem.*, 2018, **261**, 22–30.
- 24 S. B. Wu, Y. J. Ge, Y. Q. Wang, X. Chen, F. F. Li, H. Xuan and X. Li, *Environ. Technol.*, 2018, **39**, 1937–1948.
- 25 G. P. Li, S. L. Pang, Y. W. Wu and J. Ouyang, *Chem. Eng. Commun.*, 2018, **205**, 698–705.
- 26 G. Wu, J. P. Ma, S. Li, J. Guan, B. Jiang, L. Y. Wang, J. H. Li, X. Y. Wang and L. X. Chen, *J. Colloid Interface Sci.*, 2018, **528**, 360–371.
- 27 J. P. Ma, G. Wu, S. Li, W. Q. Tan, X. Y. Wang, J. H. Li and L. X. Chen, *J. Chromatogr. A*, 2018, **1553**, 57–66.
- 28 J. P. Ma, Z. D. Yao, L. W. Hou, W. H. Lu, Q. P. Yang, J. H. Li and L. X. Chen, *Talanta*, 2016, **161**, 686–692.
- 29 Y. F. Feng, H. Jiang, S. N. Li, J. Wang, X. Y. Jing, Y. R. Wang and M. Chen, *Colloids Surf., A*, 2013, **431**, 87–92.
- 30 H. Zhang, J. H. Xue, N. Hu, J. Sun, D. X. Ding, Y. D. Wang and L. Li, *J. Radioanal. Nucl. Chem.*, 2017, **308**, 865–875.
- 31 M. R. Azhar, H. R. Abid, H. Q. Sun, V. Periasamy, M. O. Tadé and S. B. Wang, *J. Colloid Interface Sci.*, 2016, **478**, 344–352.
- 32 K.-Y. A. Lin and Y.-T. Hsieh, *J. Taiwan Inst. Chem. Eng.*, 2015, **50**, 223–228.
- 33 Z. Q. Li, L. G. Qiu, T. Xu, Y. Wu, W. Wang, Z. Y. Wu and X. Jiang, *Mater. Lett.*, 2009, **63**, 78–80.
- 34 T. A. Saleh, *Nanomaterial and polymer membranes*, Elsevier, 2016, ISBN-13: 978-0128047033.
- 35 T. A. Saleh, *Advanced nanomaterials for water engineering, treatment, and hydraulics*, IGI Glob., 2017, ISBN-13: 978-1522521365.
- 36 A. W. Thornton, R. Babarao, A. Jain, F. Trouselet and F.-X. Coudert, *Dalton Trans.*, 2015, **45**, 4352–4359.
- 37 F. Zare, M. Ghaedi, A. Daneshfar, S. Agarwal, I. Tyagi, T. A. Saleh and V. K. Gupta, *Chem. Eng. J.*, 2015, **273**, 296–306.
- 38 T. A. Saleh, K. Naeemullah, M. Tuzen and A. Sari, *Chem. Eng. Res. Des.*, 2017, **117**, 218–227.
- 39 E. A. Elshehy, *Sep. Sci. Technol.*, 2017, **52**, 1852–1861.
- 40 X. Guo, Y. R. Feng, L. Ma, D. Z. Gao, J. Jing, J. C. Yu, H. B. Sun, H. Y. Gong and Y. J. Zhang, *Appl. Surf. Sci.*, 2017, **402**, 53–60.
- 41 W. Y. Wu, D. Y. Chen, J. W. Li, M. H. Su and N. Chen, *Environ. Sci. Pollut. Res.*, 2018, **25**, 18096–18108.
- 42 R. Khamirchi, A. Hosseini-Bandegharai, A. Alahabadi, S. Sivamani, A. Rahmani-Sani, T. Shahryari, I. Anastopoulos, M. Miri and H. N. Tran, *Ecotoxicol. Environ. Saf.*, 2018, **150**, 136–143.
- 43 Z. R. Dai, H. Zhang, Y. Sui, D. X. Ding, N. Hu, L. Li and Y. D. Wang, *J. Radioanal. Nucl. Chem.*, 2018, **316**, 369–382.
- 44 S. Abdi, M. Nasiri, A. Mesbahi and M. H. Khani, *J. Hazard. Mater.*, 2017, **332**, 132–139.
- 45 X. Y. Deng, Y. L. Feng, H. R. Li, F. Yuan, Q. Teng and H. J. Wang, *J. Radioanal. Nucl. Chem.*, 2018, **315**, 243–250.
- 46 J. L. Wu, K. Tian and J. L. Wang, *Prog. Nucl. Energy*, 2018, **106**, 79–86.
- 47 J. Tan, Y. F. Wang, N. Liu and M. W. Liu, *J. Radioanal. Nucl. Chem.*, 2018, **315**, 119–126.

